crystals

MDPI

Article

Crystal Growth and Glass-Like Thermal Conductivity of $Ca_3RE_2(BO_3)_4$ (RE = Y, Gd, Nd) Single Crystals

L. V. Gudzenko [1], M. B. Kosmyna [1], A. N. Shekhovtsov [1,*], W. Paszkowicz [2], A. Sulich [2], J. Z. Domagała [2], P. A. Popov [3] and S. A. Skrobov [3]

1 Institute for Single Crystals, NASU, Nauki Ave. 60, 61001 Kharkov, Ukraine; gudzenko@isc.kharkov.com (L.V.G.); kosmyna@isc.kharkov.ua (M.B.K.)
2 Institute of Physics, PAS, Aleja Lotników 32/46, PL- 02668 Warsaw, Poland; paszk@ifpan.edu.pl (W.P.); sulich@ifpan.edu.pl (A.S.); domag@ifpan.edu.pl (J.Z.D.)
3 Department of Exper. and Theor. Physics, Petrovsky Bryansk State University, Bezhitskaya Str. 14, 241036 Bryansk, Russia; tfbgubry@mail.ru (P.A.P.); skrobovsa@mail.ru (S.A.S.)
* Correspondence: shekhov@isc.kharkov.ua; Tel.: +38-057-341-0433

Academic Editors: Alain Largeteau and Helmut Cölfen
Received: 23 December 2016; Accepted: 9 March 2017; Published: 17 March 2017

Abstract: Crystal growth and thermal properties of binary borates, $Ca_3RE_2(BO_3)_4$ (RE = Y, Gd, Nd), are considered promising crystals for laser applications. These single crystals were grown by the Czochralski method. The crystal and defect structure were characterized. Volumetric chemical methods without prior separation of the components were developed and applied for the determination of the dependence of chemical compositions of the crystals on the growth conditions. The thermal conductivity was investigated in the 50–300 K range. The character of the temperature dependence of thermal conductivity was found to be similar to that of glass. The possible reasons of the observed features of the thermal conductivity were analyzed.

Keywords: binary borate; Czochralski method; crystal composition; thermal conductivity

1. Introduction

Crystal media with disordered structures (where two or more cations can share one type of site) are promising for laser application and have a number of advantages. The structure disordering leads to inhomogeneous broadening of spectral bands of the activator ions. In spite of thermal drift of light-emitting diode (LED) pumping for diodes emitting from 800 to 2000 nm, efficient pumping of the disordered medium could be achieved in the wide range of LED temperatures because of relatively wide absorption bands. Due to relatively wide luminescence bands, the wavelength of laser emission can be tuned in a wide range. For example, in a previous study [1], for disordered Nd-doped binary vanadates the duration of transform-limited pulses has been estimated to be $\Delta\tau$ = 130–160 fs at 1.07 μm. Therefore, the disordered media could also be a good solution for mode-locked lasers. $Ca_3RE_2(BO_3)_4$ (RE = rare earth element) single crystals have been considered promising materials for such an application. The transform-limited pulses of 251 fs have been generated [2].

The structure of $Ca_3RE_2(BO_3)_4$ (RE = Y, Gd) compounds is orthorhombic (space group *Pnma*) and consists of isolated BO_3 triangles, and of rare-earth (RE)–oxygen and calcium–oxygen polyhedrons. The RE cations partially occupy three non-equivalent crystallographic Ca sites. A number of papers have been published where spectral-kinetic properties of $Ca_3RE_2(BO_3)_4$ (RE = Y, Gd) crystals doped with Nd, Yb, and Er/Yb were studied [3–6]. The lasing operation under flash lamp and laser (LED and Ti/sapphire laser) pumping was also demonstrated for different regimes [2,4,7–9]. It was shown that the lasers based on these crystals are promising for many scientific tasks and practical uses. However,

investigations of these materials are at an early stage; as the thermal properties of $Ca_3RE_2(BO_3)_4$ (RE = Y, Gd) crystals have not yet been determined.

The Czochralski method is one of the most widely used ones in the industrial production of large single crystals of optical quality suitable for laser applications; for examples, see [10]. In particular, this technique was used for the growth of pure, Nd, Yb, Er/Yb-doped $Ca_3RE_2(BO_3)_4$ (RE = Y, Gd) single crystals [11]. Recently, our team has reported [12] the Czochralski growth of $Ca_3Nd_2(BO_3)_4$ crystals.

The defect structure of the given crystal may include a chemical composition inhomogeneities, mosaicity and block structure with low-angle (a fraction of degree) and large angle misorientation. The presence of such defects depends on the crystal growth technique, and on the growth conditions. The efficiency of the lasing operation depends on the crystal quality. Nowadays, the nature of the defects of the borates is not well recognized. Thus, one of the questions is related to the characterization of typical defects in $Ca_3RE_2(BO_3)_4$ (RE = Y, Gd) crystals grown by the Czochralski method.

The design of the laser apparatus (optical scheme and type of pumping), the output radiation parameters, and the operation mode depend on thermo-physical properties of the laser gain medium. Another question to be answered for the laser application of the medium is related to its thermal properties. One of the main parameters characterizing the laser gain medium is the thermal conductivity, *k*. The thermal conductivity of laser gain medium defines the temperature distribution of the active laser element and, consequently, affects the shape of the induced heat lens. Another problem is connected to achieving an effective heat removal from the active element of a high power laser.

The theories of thermal conductivity [13] could be helpful in prediction and analysis of thermal conductivity of materials suitable for lasers. However, the thermal conductivity of multicomponent material cannot be precisely calculated. The thermal conductivity of solids for the low temperature range is sensitive to defects of crystal lattice so it can serve a tool for the characterization of media. Therefore, experimental investigation of the temperature dependence taking into account the peculiarities of the crystal structure and the growth technique is of considerable scientific and practical interest.

This work is devoted to the description of the crystal growth conditions, the characterization of the chemical compositions, and the study of the thermal conductivity of $Ca_3RE_2(BO_3)_4$ (RE = Y, Gd, Nd) single crystals.

2. Experimental

$CaCO_3$ (99.99%), RE_2O_3 (99.99%) (RE = Y, Gd, Nd) and B_2O_3 (99.95%) compounds were used as reagents for the solid state synthesis of the charge. The stoichiometric mixture of the initial reagents was placed into a platinum crucible. The mixture of a total mass of 300 g was heated at the rate of 50 °C/h to 110 °C, 230 °C, 450 °C, and 750 °C and kept for 10 h at each temperature. The compound formation was carried out according to the reaction:

$$3CaCO_3 + 2B_2O_3 + RE_2O_3 \rightarrow Ca_3RE_2(BO_3)_4 + 3CO_2\uparrow.$$

The obtained material was finely ground. For crystal growth, the charge was transferred to another crucible. Pure $Ca_3RE_2(BO_3)_4$ crystals were grown by the Czochralski method using an automated and equipped with a weight control system "Kristall 3M" puller. The growth processes was carried out in inert (argon) and oxygen containing (air) atmospheres. Ir and Pt crucibles with the dimensions of a 45 mm diameter and a 50 mm length were used for argon and air atmospheres, respectively. The pulling and rotation rates were 1.5 mm/h and 20 rpm, respectively. The axial temperature gradient at the crystal-melt interface was 50 °C/cm. The crystals were grown along the [001] crystallographic axis. The crystals investigated in the present study were grown at the same conditions: at fixed temperature gradient, rotation speed, and pulling rate. The crystals had a diameter of up to 20 mm and a length of up to 90 mm (Figure 1). The grown crystals were examined by X-ray diffraction (XRD). No impurity phases and gas bubble inclusions were detected.

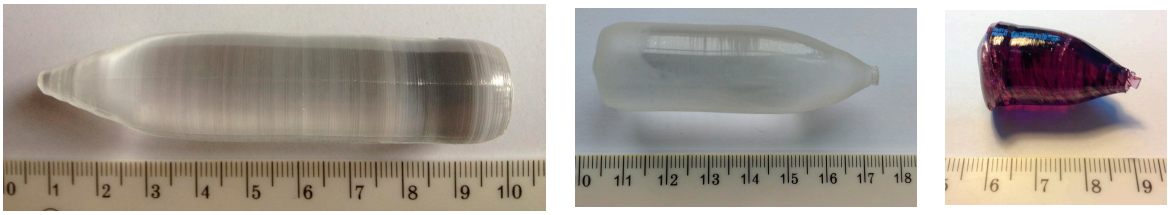

(**a**) (**b**) (**c**)

Figure 1. (**a**) $Ca_3Y_2(BO_3)_4$ crystal grown in argon from Ir crucible; (**b**) $Ca_3Gd_2(BO_3)_4$ crystal grown in air from Pt crucible; (**c**) $Ca_3Nd_2(BO_3)_4$ crystal grown in argon from Ir crucible.

The next sets of the crystals were grown: the set of $Ca_3Y_2(BO_3)_4$ crystals grown in air; the set of $Ca_3Y_2(BO_3)_4$ crystals grown in argon; the set of $Ca_3Nd_2(BO_3)_4$ crystals grown in argon; the set of $Ca_3Gd_2(BO_3)_4$ crystals grown in air; the set of $Ca_3Gd_2(BO_3)_4$ crystals grown in argon.

To determine the basic host elements of $Ca_3RE_2(BO_3)_4$ borates, volumetric chemical methods were developed. The single crystals were dissolved in a mixture of nitric and hydrochloric acids. For determination of the rare earth elements (Y or Nd, and Gd) and the calcium concentrations, the complexometric method [14] was used. For the $Ca_3Y_2(BO_3)_4$ crystal, the yttrium concentration was determined by means of ethylenediamine acetic acid sodium salt (EDTA) titration in urotropin medium containing xylenol orange indicator at 5.6–5.7 pH. In the aliquot part of the solution, the aggregated concentration of yttrium and calcium was determined using back titration of EDTA excess by zinc sulfate in ammonium chloride-buffered medium at 10 pH. The calcium content was calculated as a difference between the aggregated concentration and the Y concentration. For $Ca_3Nd_2(BO_3)_4$ and $Ca_3Gd_2(BO_3)_4$ crystals, the calcium concentration was determined by means of 1-phenyl-3-methyl-4-benzoyl-5-pyrazolone extraction. Boron was determined by means of the alkalimetric method. Yttrium, neodymium, and gadolinium were masked by the addition of EDTA. EDTA concentration was equimolar to the stoichiometric concentration of yttrium or gadolinium. The titration of boric glycerol acid was performed with a phenolphthalein indicator

Powder XRD data were collected using X'PERT MPD Alpha1 Pro diffractometer employing $CuK_{\alpha 1}$ radiation. The structures of the crystals was refined by the Rietveld method (software "Fullprof 2k v.5.30" [15]). High resolution diffraction was performed using an X'Pert MRD diffractomete equipped with primary beam optics based on an multilayer parabolic X-ray mirror and a four-bounce asymmetric Ge(022) monochromator. $CuK_{\alpha 1}$ radiation was used. The optics of the diffracted beam included a three-bounce Ge(022) analyzer.

The dependence of the thermal conductivity $k(T)$ was investigated in the range of 50–300 K by means of the method of stationary longitudinal flow. The facilities and procedure of the measurements are described in detail in [16]. To provide flatness of the isothermal surfaces, a resistive heater was fixed on the end face of the sample. The measurement error of the thermal conductivity did not exceed ±6%. The specimens for chemical analysis, XRD, and thermal conductivity study were cut from the cylindrical part of the crystal.

3. Results and Discussion

3.1. Crystal Structure

Investigation of the crystal structure of $Ca_3RE_2(BO_3)_4$ (RE = Y, Gd, Nd) borate crystals by means of powder diffraction method confirms that these crystals are of orthorhombic (space group *Pnma*). The unit cell parameters are presented in Table 1. For $Ca_3Gd_2(BO_3)_4$, and $Ca_3Nd_2(BO_3)_4$, the reciprocal space map indicate a compositional homogeneity, as no lattice parameter variation is observed. For $Ca_3Y_2(BO_3)_4$, the reciprocal space map shows a weak reflection of intensity of the order of 2% with the lattice parameter a of a higher value, 7.170 Å (Figure 2); through additional scanning the sample, it was found that this effect is due to a small misoriented grain located at the very side of the sample.

Table 1. Unit cell parameters of $Ca_3RE_2(BO_3)_4$ (RE = Y, Gd, Nd) crystals derived from powder and high-resolution (HR) XRD. The values obtained from high-resolution diffraction are given in italics; these values generally agree with those obtained from the powder diffraction; several discrepancies are attributed to the peak shifts occurring for strongly asymmetric reflections.

Crystal	*a*, Å	*b*, Å	*c*, Å	*V*, Å^3	Ref.
$Ca_3Y_2(BO_3)_4$ [a]	7.1554 (2)	15.4667 (3)	8.5583 (3)	947.15 (4)	[17]
$Ca_3Y_2(BO_3)_4$ [a]	7.1690 (4)	15.4758 (8)	8.5587 (6)	949.55 (17)	[20]
$Ca_3Y_2(BO_3)_4$ [b]	7.1517 (2) 7.152 ($)	15.4691 (4) 15.468	8.5577 (2) 8.559	946.74 (4) 946.86	this work this work HR (X)
$Ca_3Gd_2(BO_3)_4$ [a]	7.1953 (3)	15.5348 (7)	8.6197 (4)	963.49(11)	[18]
$Ca_3Gd_2(BO_3)_4$ [a]	7.1908	15.5359	8.6168	962.63	[19]
$Ca_3Gd_2(BO_3)_4$:Nd [b]	7.202	15.559	8.634	967.49	[21]
$Ca_3Gd_2(BO_3)_4$:Yb [b]	7:193 (1)	15:543 (3)	8:616 (1)	963.2 (4)	[22]
$Ca_3Gd_2(BO_3)_4$ [b]	7.1922 (2) 7.195	15.5416 (4) 15.530	8.6190 (2) 8.619	963.41 (4) 963.67	this work this work HR (Y)
$Ca_3Nd_2(BO_3)_4$ [b]	7.2384 (1) 7.230	15.7121 (2) 15.713	8.6666 (1) 8.665	985.66 (2) 985.45	this work this work HR (Z)

[a]: the X-ray diffraction data for the compound produced by solid state synthesis; [b]: the X-ray diffraction data for the ground single crystal. (X): calculated from positions of 600, 462, and 606 reflections (Figure 2). (Y): calculated from positions of 512, 048, and 006 reflections at the reciprocal space map (Figure 2). (Z): calculated from positions of **6 5 2**, **0 18 0**, and **0 15 5** reflections at the reciprocal space map (Figure 2). ($) Data for a small grain located at a sample side.

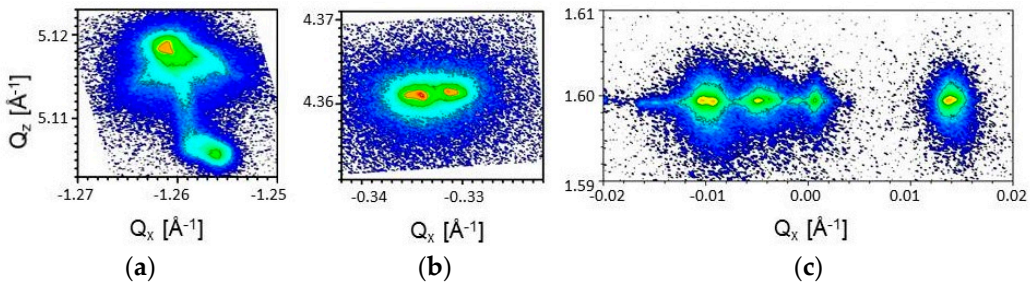

Figure 2. Reciprocal space maps for: 600 reflection of $Ca_3Y_2(BO_3)_4$ (**a**); 006 reflection of $Ca_3Gd_2(BO_3)_4$ (**b**); 040 reflection of $Ca_3Nd_2(BO_3)_4$ (**c**).

As can be seen from Table 1, the unit cell size has been observed to increase with an increasing size of RE cation (the ionic radius, R_Y (1.019 Å) → R_{Nd} (1.053 Å) → R_{Gd} (1.109 Å)). The parameters of unit cell of $Ca_3RE_2(BO_3)_4$ crystals differ marginally from those available in the literature for RE = Y [17] and RE = Gd [18,19]; data for RE = Nd have not been reported yet. A comparison of lattice parameter variation among the (sparse) experimental results of different laboratories show that the range of their relative values is about 0.5% (the changes are larger for doped crystals). These variations express the influence of factors such as material purity, composition, and preparation. In particular, the Czochralski growth technique could lead to some excess from the stoichiometry of the grown crystal, visible in the lattice parameter values. In the present study, the discrepancies are marginal and do not indicate significant composition changes.

The high-resolution diffraction shows small differences in the macroscopic defect structure of the three crystals. The samples were circular plates cut vertically to the growth axis (RE = Y and Gd) and parallel to the axis (RE = Nd). The rocking curves measured for areas of about 20 mm^2 for $Ca_3RE_2(BO_3)_4$ have FWHM values of 71.5″, 51.8′, and 146.3″ for RE = Y, Gd, and Nd, respectively (Figure 3), showing that as for the block structure, mosaicity and homogeneity, the best crystal among the studied ones is $Ca_3Gd_2(BO_3)_4$. The $Ca_3Gd_2(BO_3)_4$ and $Ca_3Nd_2(BO_3)_4$ crystal demonstrate a fully uniform composition; for both, in the irradiated area of the sample, a presence of more than one crystal block is observed. For $Ca_3Gd_2(BO_3)_4$, a difference in orientation discrepancy of the two blocks is 0.04°;

the second block is of a minor size (<5% of the irradiated surface). For the $Ca_3Nd_2(BO_3)_4$ crystal, four monocrystalline blocks were observed with misorientations ranging up to 1.5° (here, the block structure can be observed by eye). For $Ca_3Y_2(BO_3)_4$, two blocks are found with misorientation of about 0.1°. However, the second block is a very small grain (the area of about 2%) located at the very side of the crystal sample. The difference in 2θ is 0.25°; the small grain has a larger value of lattice parameter *a*.

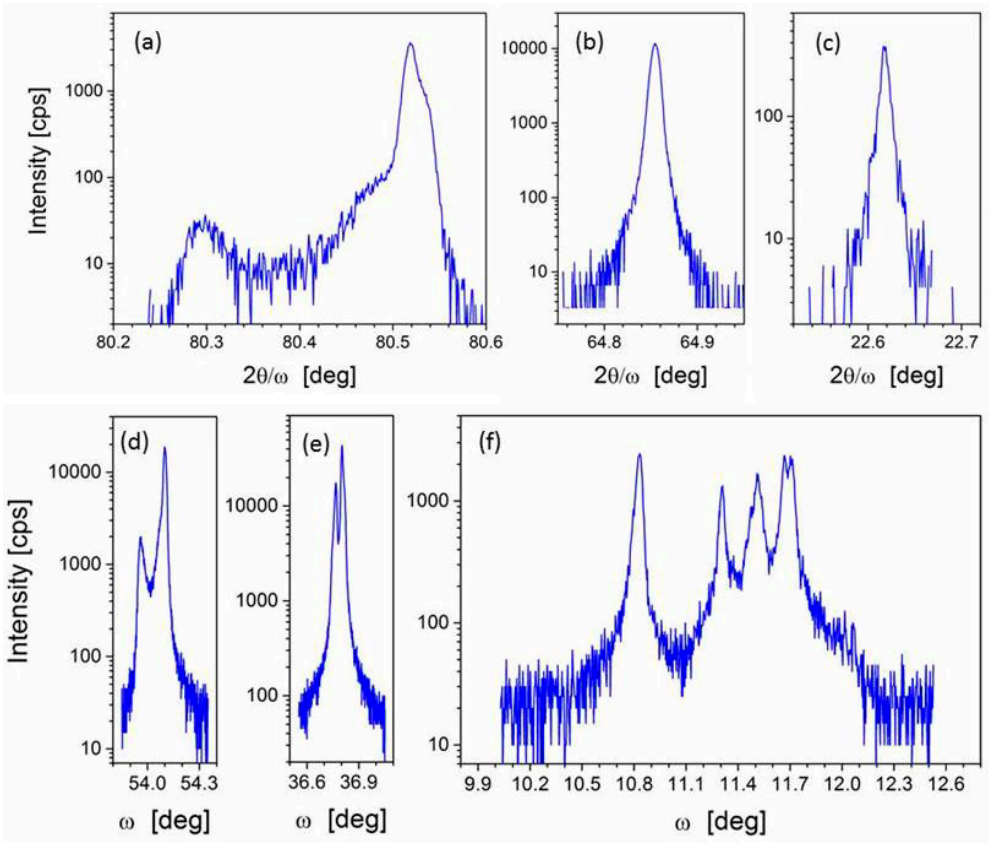

Figure 3. Logarithmic intensity scale $2\theta/\omega$ and ω scans for 600 reflection of $Ca_3Y_2(BO_3)_4$ (**a** and **d**, respectively), 006 reflection of $Ca_3Gd_2(BO_3)_4$ (**b** and **e**, respectively), 040 reflection of $Ca_3Nd_2(BO_3)_4$ (**c** and **f**, respectively). The logarithmic scale strongly enhances the minor effects of secondary grains and compositional inhomogeneity observed in $Ca_3Y_2(BO_3)_4$ (left), and $Ca_3Gd_2(BO_3)_4$.

3.2. Chemical Composition

Since the thermal conductivity of solids for the low temperature range is sensitive to defects of crystal lattice, the chemical analysis of the grown crystals could be performed. According to the chemical analysis date for all crystals grown both in argon and air atmospheres, the deviation from the stoichiometric composition was determined. The goal of this analysis was to check the excess or deficit of cationic components (a deviation from stoichiometry would be an indicator of point defect presence). In particular, the deviation of the Ca/RE ratio from the stoichiometric one and the boron deficit were studied.

For all $Ca_3Y_2(BO_3)_4$ crystals grown both in argon and air atmospheres, the Ca/Y ratio fluctuated in the frames of 10 wt %, the boron deficit did not exceed 0.5 wt % at the accuracy of measurements ±0.1 wt %. For $Ca_3Nd_2(BO_3)_4$ crystals grown in argon, the deviation of the Ca/Nd ratio did not exceed 6 wt % and the boron concentration was close the stoichiometric one. For all $Ca_3Gd_2(BO_3)_4$ crystals grown both in argon and air atmospheres, the deviation of the Ca/Gd ratio reached 7 wt %. The boron deficit was in the 0–0.3 wt % range. These observations coincide with those from high-resolution diffraction, described in the above paragraph.

Moreover, for the $Ca_3Y_2(BO_3)_4$ crystal with the length of 90 mm grown in argon, the distribution of the host element was investigated. The measurements of the host element content were made with a 1 cm step and the inhomogeneous composition of the crystal grown under these conditions was established. The maximum deviation from the stoichiometric Ca/Y ratio was observed for the upper (no more 5%) and bottom (up to 9%) cones of the crystal. For the cylindrical part of the crystal, the deviation was in frames of 3%. The minor boron deficit was observed, but the boron content did not vary along the crystal.

For all crystals grown, both in argon and air, the observed deviation of the Ca/RE ratio from the stoichiometric composition leads to the deficit of positive charge. Obviously, for compensation of the positive charge deficit, the defects in the anion sublattice should be formed: $[B_{4-x}(V_B)_xO_{12-y}(V_O)_y]$, where V_B and V_O are the boron and oxygen vacancies, respectively. According to the chemical analysis data, the boron deficit was determined for $Ca_3RE_2(BO_3)_4$ (RE = Y, Gd) crystal grown both in argon and air. The boron deficit grew for the crystals grown in air. Obviously, the oxygen vacancies dominate in the crystals grown in argon. The concentration of boron vacancies is higher in the crystals grown in air due to more intense boron evaporation from the surface of the melt in the medium containing acid vapors (air) [23].

Thus, the typical defect of the crystal grown by direct crystallization from the melt by means of the Czochralski method is the deviation from the stoichiometric composition. The $Ca_3RE_2(BO_3)_4$ (RE = Y, Gd, and Nd) crystals grown in argon with the composition the closest to the stoichiometric one chosen for the thermal conductivity study. Their element composition is presented in Table 2. For comparison, the concentrations of host elements for the best $Ca_3RE_2(BO_3)_4$ (RE = Y, Gd) crystals grown in air atmosphere sets are also shown.

Table 2. Concentrations of host elements for $Ca_3RE_2(BO_3)_4$ (RE = Y, Gd, Nd) crystals.

Crystal	Host Element Concentrations, wt %			
		RE	Ca	B
$Ca_3Y_2(BO_3)_4$	Stoichiometrically calculated content	33.3	22.5	8.1
	Grown in argon	33.3 ± 0.1	22.3 ± 0.1	7.9 ± 0.1
	Grown in air	33.4 ± 0.1	22.2 ± 0.1	7.6 ± 0.1
$Ca_3Gd_2(BO_3)_4$	Stoichiometrically calculated content	46.9	17.9	6.5
	Grown in argon	46.8 ± 0.1	18.0 ± 0.1	6.5 ± 0.1
	Grown in air	45.8 ± 0.1	18.2 ± 0.1	6.4 ± 0.1
$Ca_3Nd_2(BO_3)_4$	Stoichiometrically calculated content	44.8	18.7	6.7
	Grown in argon	44.4 ± 0.1	19.5 ± 0.1	6.8 ± 0.1

3.3. Thermal Conductivity

Unexpectedly, the temperature dependences $k(T)$ of $Ca_3RE_2(BO_3)_4$ (RE = Y, Gd, Nd) crystals, $k(T)$, is found to be typical for fully disordered media, e.g., glass, but not for ordered ones (crystals). The absolute values of the obtained thermal conductivity are also typical for glass. At room temperature, they are within a narrow range between 0.9 ± 0.05 W/(m·K) and 1.04 ± 0.06 W/(m·K). (Figure 4).

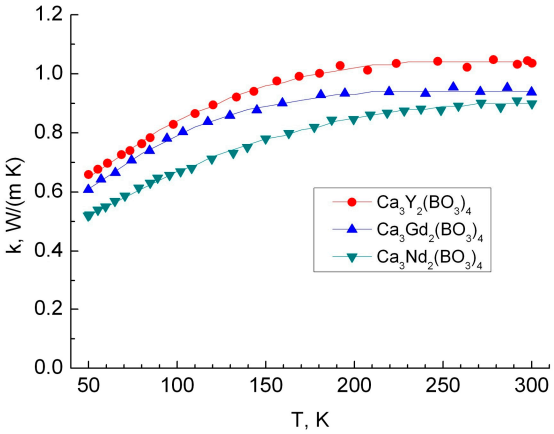

Figure 4. Temperature dependence of the thermal conductivity *k*(T) for $Ca_3RE_2(BO_3)_4$ (RE = Y, Gd, Nd) crystals along the *c* axis.

The temperature dependences k(T) was approximated by the polynomial:

$$k(T) = AT^3 + BT^2 + CT + D. \quad (1)$$

The A, B, C, and D coefficients for the investigated crystals are quoted in Table 3. The change over from one cation to the cations with another mass and ionic radius does not essentially affect neither the absolute value nor the temperature behavior of the thermal conductivity.

Table 3. A, B, C, and D coefficients of Equation (1) describing the thermal conductivity of $Ca_3RE_2(BO_3)_4$ (RE = Y, Gd, Nd) crystals.

	A, 10^{-8} W/(m·K^4)	B, 10^{-5} W/(m·K^3)	C, 10^{-3} W/(m·K^2)	D, W/(m·K)
$Ca_3Y_2(BO_3)_4$	1.75	−1.889	6.27	0.382
$Ca_3Gd_2(BO_3)_4$	0.4031	−0.8876	4.184	0.334
$Ca_3Nd_2(BO_3)_4$	3.295	2.646	7.067	0.316

The monotonic increasing dependences *k*(T) may be interpreted as follows. According to generally accepted ideas of phonon heat transfer, the thermal conductivity may be presented by the Debye expression:

$$k = C\,l\,v/3 \quad (2)$$

where *C* is the heat capacity of a unit of volume, v is the average velocity of sound phonon propagation, and *l* is the average length of phonon free path [24]. At the intense phonon scattering on the structure defects, *l* approaches its least value and depends slightly on the temperature. Because the sound velocity weakly depends on the temperature, the rise of heat capacity at rather low temperatures defines the increase in the thermal conductivity.

The $Ca_3RE_2(BO_3)_4$ (RE = Y, Gd, Nd) crystals have practically the same value of thermal conductivity, therefore we may conclude that the substitution of RE cations does not essentially affect phonon scattering in comparison with the intense phonon scattering on other structure inhomogeneities. The same temperature behavior of thermal conductivity and the low values of thermal conductivity of ~1 W (m·K) at room temperature were observed for binary $Ca_9RE(VO_4)_7$ (RE = La, Nd, Gd) vanadate crystals, which are also characterized by the inhomogeneous composition [25]. The thermal conductivity of the crystal is directly connected with its thermal capacity and elastic characteristics. Thus, we can conclude that these parameters are almost identical for the investigated crystals.

4. Conclusions

Thermal conductivity is one of the factors influencing the laser applications of oxide crystals. In this work, we studied the properties of Czochralski-grown $Ca_3RE_2(BO_3)_4$ (RE = Y, Gd, Nd) borate single crystals. Their composition and structural properties and quality were characterized by analytical methods. The volumetric analytical chemistry methods were developed and applied for the determination of the chemical compositions. The crystals grown both in argon and air atmosphere are characterized by some deviation of the Ca/RE ratio from the stoichiometric composition and a minor boron deficit. The high-resolution X-ray diffraction results indicate that the studied $Ca_3Y_2(BO_3)_4$ and $Ca_3Gd_2(BO_3)_4$ are of good quality, whereas the $Ca_3Nd_2(BO_3)_4$ crystal is built from several blocks misoriented by up to 1.5°. Further work is needed in order to more deeply analyze the influence of growth parameters on the homogeneity and mosaicity of the borate crystals.

The temperature dependences of the thermal conductivity for the $Ca_3RE_2(BO_3)_4$ (RE = Y, Gd, Nd) crystals are studied. The conductivity decreases with rising temperature, the absolute values become smaller across the Y, Gd, and Nd series, and the change is of the order of 15%. The absolute value and the character of the temperature dependence of the thermal conductivity are similar to those known for glasses. The values of thermal conductivity make these materials suitable for consideration as potential laser materials suitable for heat dissipation during laser action.

Author Contributions: Alexey Shekhovtsov conceived the project and prepared the manuscript; Miron Kosmyna and Alexey Shekhovtsov performed the crystal growth; Ludmila Gudzenko performed the chemical analysis; Wojciech Paszkowicz, Jarosław Z Domagała, Adrian Sulich carried out the X-ray diffraction studies; Pavel Popov and Sergey Skrobov studied the thermal conductivity; all authors contributed to discussion and analysis of obtained results.

Conflicts of Interest: The authors declare no conflict of interest. The founding sponsors had no role in the design of the study; in the collection, analyses, or interpretation of data; in the writing of the manuscript; or in the decision to publish the results.

References and Notes

1. Loiko, P.A.; Yasukevich, A.S.; Gulevich, A.E.; Demesh, M.P.; Kosmyna, M.B.; Nazarenko, B.P.; Puzikov, V.M.; Shekhovtsov, A.N.; Kornienko, A.A.; Dunina, E.B.; et al. Growth, spectroscopic and thermal properties of Nd-doped disordered $Ca_9La(VO_4)_7$ and $Ca_{10}(Li/K)(VO_4)_7$ laser crystals. *J. Lumin.* **2013**, *137*, 252–258. [CrossRef]
2. Pan, Z.; Ma, J.; Xu, H.; Tang, D.; Cai, H.; Yu, H.; Zhang, H.; Wange, J. 251 fs pulse generation with a Nd^{3+}-doped $Ca_3Gd_2(BO_3)_4$ disordered crystal. *RSC Adv.* **2012**, *5*, 44137–44141. [CrossRef]
3. Mill, B.V.; Tkachuk, A.M.; Belokoneva, E.L.; Ershova, G.I.; Mironov, D.I.; Razumova, I.K. Spectroscopic studies of $Ln_2Ca_3B_4O_{12}$-Nd (Ln-Y, La, Gd) crystals. *J. Alloys Compd.* **1998**, *275–277*, 291–294. [CrossRef]
4. Haumesser, P.H.; Gaume, R.; Viana, B.; Vivien, D. Determination of laser parameters of ytterbium doped oxide crystalline materials. *J. Opt. Soc. Am. B* **2002**, *19*, 2365–2375. [CrossRef]
5. Wei, B.; Hu, Z.; Lin, Z.; Zhang, L.; Wang, G. Growth and spectral properties of Er^{3+}/Yb^{3+}-codoped $Ca_3Y_2(BO_3)_4$ crystal. *J. Cryst. Growth* **2004**, *273*, 190–194. [CrossRef]
6. Wang, Y.; Tu, C.; You, Z.; Li, J.; Zhu, Z.; Jia, G.; Lu, X.; Wu, B. Optical spectroscopy of $Ca_3Gd_2(BO_3)_4$:Nd^{3+} laser crystal. *J. Mod. Opt.* **2006**, *53*, 1141–1148. [CrossRef]
7. Brenier, A.; Tu, C.; Wang, Y.; You, Z.; Zhu, Z.; Li, J. Diode-pumped laser operation of Yb^{3+}-doped $Y_2Ca_3B_4O_{12}$ crystal. *J. Appl. Phys.* **2008**, *104*, 013102–013105. [CrossRef]
8. Ji, Y.; Wang, Y.; Cao, J.; You, Z.; Wang, Y.; Tu, C. Spectroscopic analysis of Nd^{3+}:$Ca_3Gd_2(BO_3)_4$ crystal and laser operating at 1.06 μm. *J. Alloys Compd.* **2011**, *509*, 9753–9757. [CrossRef]
9. Kosmyna, M.B.; Nazarenko, B.P.; Radchenko, I.O.; Shekhovtsov, A.N. Characteristics of lasers based on binary vanadate and orthoborate single crystals with disordered structure. *Funct. Mater.* **2015**, *22*, 446–449. [CrossRef]
10. Kosmyna, M.B.; Nazarenko, B.P.; Puzikov, V.M.; Shekhovtsov, A.N. Development of growth technologies for the photonic single crystals by the Czochralski method at Institute for Single Crystals, NAS of Ukraine. *Acta Phys. Pol. A* **2013**, *123*, 305–313. [CrossRef]

11. Tu, C.; Wang, Y. The Recent Development of Rare Earth-Doped Borate Laser Crystals. In *Solid State Laser*; Al-Khursan, A., Ed.; INTECH Open Access Publisher: Rijeka, Croatia, 2012; pp. 63–118.
12. Gudzenko, L.V.; Kosmyna, M.B.; Paszkowicz, W.; Shekhovtsov, A.N.; Behrooz, A.; Białogłowski, M. Growth and characterization of disordered double borate laser hosts. In Proceedings of the 5th International Workshop on Directionally Solidified Eutectic Ceramics, Warsaw, Poland, 3–7 April 2016.
13. Berman, R. *Thermal Conduction in Solids*; Clarendon Press: Oxford, UK, 1976.
14. Schwarzenbach, G.; Flaschka, H. *Die Komplexometrische Titration*; Ferdinand Enke Verlag: Stuttgart, Germany, 1965. (In German)
15. Rodriguez-Carvajal, J. FULLPROF: A program for Rietveld refinement and pattern matching analysis. In Proceedings of the Satellite Meeting on Powder Diffraction of the XV Congress of the IUCr, Toulouse, France, 16–19 July 1990.
16. Sirota, N.N.; Popov, P.A.; Ivanov, I.A. The Thermal Conductivity of Monocrystalline Gallium Garnets Doped with Rare-Earth Elements and Chromium in the Range 6–300 K. *Cryst. Res. Technol.* **1992**, *27*, 535–543. [CrossRef]
17. Ivanov, S.; Zhurov, V.Y. ICDD Database **2000**, PDF480310.
18. Ivanov, S.; Zhurov, V.Y. ICDD Database **2000**, PDF480293.
19. Seo, H.J. Line broadening and crystallographic sites for Eu^{3+} in disordered double borate $Ca_3Gd_2(BO_3)_4$. *J. Alloys Compd.* **2014**, *604*, 100–105. [CrossRef]
20. Dzhurinskiy, B.F.; Tanaev, N.V.; Aliev, O.A. Solubility and phase equilibria in systems Sm_2O_3-SrO-B_2O_3 and Eu_2O_3-SrO-B_2O_3. *Inorg. Mater.* **1968**, *4*, 1972–1975. (In Russian)
21. Pan, Z.B.; Zhang, H.J.; Yu, H.H.; Xu, M.; Zhang, Y.Y.; Sun, S.Q.; Wang, J.Y.; Wang, Q.; Wei, Z.Y.; Zhang, Z.G. Growth and characterization of Nd-doped disordered $Ca_3Gd_2(BO_3)_4$ crystal. *Appl. Phys. B Lasers Opt.* **2012**, *106*, 197–209. [CrossRef]
22. Haumesser, P.H.; Gaumé, R.; Benitez, J.M.; Viana, B.; Ferrand, B.; Aka, G.; Vivien, D. Czochralski growth of six Yb-doped double borate and silicate laser materials. *J. Crystal Growth* **2001**, *233*, 233–242. [CrossRef]
23. Nemodruk, A.A.; Karalova, Z.K. *Analytical Chemistry of Boron*; Nauka: Moscow, Soviet Unoin, 1964. (In Russian)
24. Debye, P. *Vortrage uber die Kinetische Theorie der Materie and der Elektrizitat*; B.G. Teubner: Berlin, Germany, 1914.
25. Popov, P.A.; Skrobov, S.A.; Matovnikov, A.V.; Kosmyna, M.B.; Puzikov, V.M.; Nazarenko, B.P.; Shekhovtsov, A.N.; Behrooz, A.; Paszkowicz, W.; Khodasevich, I.A.; et al. Thermal conductivity investigation of $Ca_9RE(VO_4)_7$ (RE = La, Nd, Gd) and $Ca_{10}M(VO_4)_7$ (M = Li, Na, K) single crystals. *Int. J. Thermophys.* **2017**, *38*, 13.